

Power Quality Enhancement in Double Fed Induction Generator Using Iterative Learning Control

Abstract. This paper presents a combination of the proposed Sliding Mode Control and a newly developed iterative learning control technique for harmonic compensation for the fault's effect to adjust the active and reactive power to their desired references. The classical SMC cannot deal with the effect of the faults that can achieve graceful system degradation. Indeed, when there are significant disturbances, the input control signal of the SM controller is gradually adjusted by the ILC harmonic compensator in order to reject the disruptive harmonics effectively. Simulation results are given to demonstrate the effectiveness of the suggested SMC-ILC in terms of active and reactive power responses. The obtained results illustrate that the SMC-ILC strategy is valid and capable of ensuring a ripple-free operation in the presence of faults. The proposed controller is characterized by its simple design, robustness, and efficiency, which are convincing for practical application and may be used as a solution to the current Fault Tolerant Control.

Streszczenie. W artykule przedstawiono kombinację proponowanej regulacji trybu ślizgowego i nowo opracowanej techniki iteracyjnego sterowania z uczeniem w celu kompensacji harmonicznych w obecności zwarć, aby sterować mocą czynną i bierną zgodnie z ich pożądanymi wartościami odniesienia. Klasyczny SMC nie radzi sobie ze skutkami usterek, które mogą doprowadzić do płynnej degradacji systemu. Rzeczywiście, gdy występują znaczne zakłócenia, wejściowy sygnał sterujący kontrolera SM jest stopniowo regulowany przez kompensator harmonicznych ILC w celu skutecznego odrzucenia zakłócających harmonicznych. Przedstawiono wyniki symulacji, aby pokazać skuteczność proponowanego SMC-ILC w zakresie odpowiedzi mocy czynnej i biernej. Uzyskane wyniki pokazują, że strategia SMC-ILC jest poprawna i zdolna do zapewnienia działania bez tętnień w przypadku wystąpienia usterki. Proponowany sterownik charakteryzuje się wytrzymałością, wydajnością i prostą konstrukcją, które przekonują do praktycznego zastosowania i mogą być stosowane jako alternatywa dla dotychczasowych Kontrola odporna na awarie. (Poprawa jakości energii w generatorze indukcyjnym z podwójnym zasilaniem przy użyciu iteracyjnej kontroli uczenia)

Keywords: Doubly Fed Induction Generator (DFIG), Fault Tolerant Control (FTC), Sliding Mode Control (SMC), Iterative Learning Control (ILC).

Słowa kluczowe: generator indukcyjny z podwójnym zasilaniem (DFIG), Kontrola odporności na awarie (FTC), kontrola trybu ślizgowego (SMC), sterowanie iteracyjne (ILC).

1. Introduction

In the last ten years, many countries have increased the demand for wind energy for developing their economies with several energy conversion machines (WECMs) [1]; one major of these machine

s is the doubly-fed induction generator (DFIG). During the last decade, the doubly-fed induction generator (DFIG) has become more appealing (used) and

popular due to its advantages over other generators, such as better controlling skills, fully variable speed operation, low maintenance, robustness, and reduced inverter costs [2-3]. Despite these advantages, many types of faults affect this kind of generator, such as short-circuit faults, speed sensor faults, DC voltage overshoot faults, grid faults, and actuator faults [4]. These faults must be considered to ensure the proper operation of the system. Different techniques have been reported and investigated to overcome these thresholds in this context. One of them is called Fault-tolerant control (FTC) [5].

In recent years, the fault-tolerant control approach has received worldwide attention because it enables a system to continue working properly in the event of faults [2]. This approach can be classified into two types: Passive and Active Fault-Tolerant Control [6-7]. PFTC employs robust control approaches to ensure system insensitivity to closed-loop failures. While keeping the same controller and structure [8]. Otherwise, AFTC aims to adjust the stability and performance, in case of degradation, because of the post-fault model, by modifying online the parameters or the structure of the controller. This solution requires to be reconfigured based on the block information given for fault detection and isolation on (FDI) [9-10-11-12].

Over the last few decades, many researchers have focused on sliding mode control to handle systems under faults. This control has the advantage of ensuring the robustness of disturbed systems by reducing the impacts of external disturbances to the appropriate level [13-14].

Therefore, the authors in [15] propose an integral sliding mode controller to minimize the disturbance terms that affect nonlinear systems with the state-dependent importance and the input matrix. However, this technique has certain disadvantages; one is the chattering effect. That is produced by the discontinuous component of this command, which might be harmful to the actuators. In order To eliminate the shortcoming, different decomposition strategies are presented in some studies [16-7]. The [16] develops An efficient fault detection, reconstruction and fault-tolerant control approach (FTC) for induction motors with usual defects. It is demonstrated that this technique is based on sliding mode control that can adjust the stability of the closed-loop system and steer the system's output to their desired reference.

Nevertheless, this controller cannot handle directly complete system failures. To overcome this issue, they proposed a combination between SMC and sliding mode observer (SMO) to detect and reconstruct the faults. Furthermore, the authors in [7] present an appropriate combination of the SMC and a fault detection and compensation block for a double-star induction machine to make the speed and the flux follow their desired references.

Based on the previously mentioned references, the power quality enhancement in a doubly-fed induction generator is still a challenging task. Hence, this paper presents an efficient Fault Tolerant Control (FTC) strategy for power quality enhancement in a doubly-fed induction generator. The suggested approach combines a sliding mode controller (SMC) with an iterative learning controller (ILC) for ripple attenuation created by rotor faults. This strategy is adapted for industrial power applications because of its effectiveness and robustness during critical process situations. In this subject, many researchers have been attracted to ILC techniques in applications subjected to continual periodic disturbances; this scheme can repeatedly alter the control signal when the control task is

performed to obtain high disturbance rejection [17-18]. In [17], two iterative learning control techniques applied in the time and frequency domains have been presented to minimize periodic speed ripples caused by torque pulsations; both control techniques have the same drive configuration. A combination of the proposed iterative learning control (ILC) and the traditional PI speed controller is applied, which serves as the significant reference current. The authors in [18] develop a practical control approach for improving power quality in a standalone system based on a four-leg inverter. The suggested controller combines a sliding mode controller (SMC) with an iterative learning controller (ILC) for harmonic compensation. Several contributions can be described in this work:

- In [19,20], authors offer a complicated FTC structure-based projection approach, which requires a switching block (to switch between two control techniques). In this study, we suggest a straightforward Fault Tolerant Control structure based on SMC with iterative learning control, which can operate without a switching block.

- Compared to [21-22], the severity of the fault addressed in this work is more significant because open-phase fault tolerance is a particular aspect of multiphase machines due to a large number of related phases.

- Compared to the work in [12], applying the proposed FTC to DFIG is more beneficial because the multiphase induction machine is now more commonly utilised as a centrepiece in different essential areas of industry than the traditional induction motor.

This paper is structured as follows: First, Section 2 establishes the DFIG healthy model. Section 3 describes an SMC control for active and reactive power controls. Section 4 details the defective model of DFIG. The proposed ILC scheme is presented in Section 5. The simulation results of the closed-loop system are presented in Section 6. Section 7 gives a conclusion.

2. DFIG Healthy Model

The mathematical model of DFIG in the park is provided by the equations below. [3-23]:

$$(1) \quad \begin{cases} V_{ds} = R_s I_{ds} + \frac{d}{dt} \varphi_{ds} - w_s \varphi_{qs} \\ V_{qs} = R_s I_{qs} + \frac{d}{dt} \varphi_{qs} + w_s \varphi_{ds} \\ V_{dr} = R_r I_{dr} + \frac{d}{dt} \varphi_{dr} - w_r \varphi_{qr} \\ V_{qr} = R_r I_{qr} + \frac{d}{dt} \varphi_{qr} + w_r \varphi_{dr} \end{cases}$$

$$(2) \quad \begin{cases} \varphi_{ds} = L_s I_{ds} + M I_{dr} \\ \varphi_{qs} = L_s I_{qs} + M I_{qr} \\ \varphi_{dr} = L_r I_{dr} + M I_{ds} \\ \varphi_{qr} = L_r I_{qr} + M I_{qs} \end{cases}$$

$$(3) \quad C_{em} = p \frac{M}{L_s} (I_{rd} \varphi_{qs} - I_{qr} \varphi_{ds})$$

Where: R_s and R_r are the stator and rotor resistance, L_s and L_r are the stator and rotor inductances, M is the mutual inductance, I_{dr} , I_{qr} are rotor current components, I_{ds} , I_{qs} are stator current components,

V_{ds} , V_{qs} are stator voltage components, V_{dr} , V_{qr} are rotor voltage components, φ denote magnetic flux, w_s Represents the synchronous speed, and indexes d, q stand for the direct and quadrature components.

$$(4) \quad \begin{cases} \frac{dI_{ds}}{dt} = -a_0 I_{ds} + b_1 w_s I_{qs} - a_1 I_{qs} + a_2 R_r I_{dr} - a_3 w_r I_{qr} + a_3 w_s I_{qr} + b_0 V_{ds} - a_2 V_{dr} \\ \frac{dI_{qs}}{dt} = -a_0 I_{qs} + b_1 w_s I_{ds} + a_1 w_r I_{ds} + a_3 w_r I_{dr} + a_2 R_r I_{qr} - a_3 w_s I_{dr} + b_0 V_{qs} - a_2 V_{qr} \\ \frac{dI_{dr}}{dt} = a_5 I_{ds} - a_6 w_s I_{qs} + a_6 w_r I_{qs} - b_2 R_r I_{dr} + b_1 w_r I_{qr} - a_4 w_s I_{qr} - a_7 V_{ds} + b_2 V_{dr} \\ \frac{dI_{qr}}{dt} = a_6 w_s I_{ds} - a_6 w_r I_{ds} + a_5 I_{qs} + a_4 w_s I_{dr} - b_1 w_r I_{dr} - b_2 R_r I_{qr} - a_7 V_{qs} + b_2 V_{qr} \end{cases}$$

Where:

$$\begin{cases} a_0 = \frac{R_s}{\sigma L_s}, a_1 = \frac{M^2 w_r}{L_r L_s \sigma}, a_2 = \frac{M}{L_r L_s \sigma}, a_3 = \frac{M}{L_s \sigma}, \\ a_5 = \frac{M R_s}{L_r L_s \sigma}, a_4 = \frac{M^2}{L_r L_s \sigma}, a_6 = \frac{M}{L_r \sigma}, a_7 = \frac{M}{L_r L_s \sigma} \\ b_0 = \frac{1}{\sigma L_s}, b_1 = \frac{1}{\sigma}, b_2 = \frac{1}{\sigma L_r}, \sigma = \frac{1-M^2}{L_s L_r} \end{cases}$$

The Active and reactive stator powers equations are:

$$(5) \quad \begin{cases} P_s = \frac{3}{2} (V_{ds} I_{ds} + V_{qs} I_{qs}) \\ Q_s = \frac{3}{2} (V_{qs} I_{ds} - V_{ds} I_{qs}) \end{cases}$$

3. Sliding mode control

In modern control principles, Sliding Mode Control (SMC) theory is a vital control technique in terms of robustness and simple realization [16] because of its order reduction, disruption exclusion, high robustness, and easy implementation via power converter. More information on the sliding mode can be found in [24-25-26]. As stated in [3], the architecture of the sliding mode controller considers device stability and systematically accounts for stability and good performance. Here, complete design steps are given for the sliding mode controller.

3.1. Sliding surface design

We can give the surface $S(x)$ as:

$$(6) \quad S(x) = \left(\lambda + \frac{d}{dt} \right)^{r-1} (x_{ref} - x)$$

Where:

x , x_{ref} are the state and the reference variable, r , λ are the sliding mode's degree and the weighting component.

Active power is directly related to the q-axis rotor current, while reactive power is related to the d-axis rotor current.

Therefore, the expression of active and reactive powers control surfaces becomes as follows:

$$(7) \quad s(P) = (I_{qr}^{ref} - I_{qr})$$

$$(8) \quad s(Q) = (I_{dr}^{ref} - I_{dr})$$

In order to adjust the convergence of the reference variables. The following equation scheme must be verified.

$$(9) \quad \begin{cases} s(P) = 0 \\ s(Q) = 0 \end{cases} \Rightarrow \begin{cases} \frac{d}{dt}(I_{qr}^{ref} - I_{qr}) = 0 \\ \frac{d}{dt}(I_{dr}^{ref} - I_{dr}) = 0 \end{cases}$$

Consequently, the active and reactive power must converge to their references exponentially for a zero-sliding surface $s(P, Q)$. So, in order to monitor P_{sref} and Q_{sref} , it is necessary to make the sliding surface attractive and unchangeable.

Testing the attractiveness relationship of Lyapunov is conditional on the effectiveness of sliding mode regulation, given by:

$$(10) \quad s(X) \cdot \dot{s}(X) \leq 0$$

3.2. SMC Algorithm

The third stage is the derivation of control laws that allows the controlled variables to be held very close to the sliding surface.

In order to enhance the dynamic efficiency, the control voltage vectors can be described by the following formulas:

$$(11) \quad \begin{cases} V_{qr} = V_{qr_eq} + V_{qr_N} \\ V_{dr} = V_{dr_eq} + V_{dr_N} \end{cases}$$

$$(12) \quad \begin{cases} V_{qr_N} = -k_1 \cdot \text{sign}(s(p)) \\ V_{dr_N} = -k_2 \cdot \text{sign}(s(p)) \end{cases}$$

$V_{qr} V_{dr}$: is the control vector, V_{qr_eq} , V_{dr_eq} are equivalent control obtained by setting $\dot{s}(t) = 0$, and the function of equivalent control is to preserve the system on the sliding surface defined by $S(t) = 0$.

V_{qr_N} , V_{dr_N} are the switching control; they converge the direction of the device towards the sliding surface.

A continuous function expressed by (13) determines the regulated variables' maximum and minimum excursion values by using a sign function to minimize the chattering effect.

$$(13) \quad \text{sign}(S(x)) = \begin{cases} -1 & \text{if } S(x) < 0 \\ 1 & \text{if } S(x) > 0 \end{cases}$$

$$(14) \quad V_{dqr_N} = k_x \frac{S(x)}{|S(x)| + m}$$

Where: m is a minimal positive scalar, and k_x is a constant.

3.3. Application of the SMC on DFIG

a) Active Power Control

We put $r=1$ (The control law is determined by the relative degree of the number of derivative times of the control surface) to control active power, thus the control surface expression and its derivative for the control of active power are defined by:

$$(15) \quad s(P) = (I_{qr}^{ref} - I_{qr})$$

$$(16) \quad \dot{s}(P) = (\dot{I}_{qr}^{ref} - \dot{I}_{qr})$$

By replacing \dot{I}_{qr}^{ref} and \dot{I}_{qr} with their relative expressions, we can obtain:

$$(17) \quad \dot{s}(p) = \begin{pmatrix} -\frac{L_s}{M \cdot V_s} \dot{P}_s^{ref} - \frac{1}{L_r \sigma} \\ V_{qr} - R_r \cdot I_{qr} - g \cdot w_s L_r \sigma I_{dr} - \\ -g \frac{M \cdot V_s}{L_s} - h_2(x) \end{pmatrix}$$

$$(18) \quad \dot{s}(p) = \begin{pmatrix} -\frac{L_s}{M \cdot V_s} \dot{P}_s^{ref} - \frac{1}{L_r \sigma} V_{qr} - \frac{1}{L_r \sigma} \\ R_r I_{qr} - g \cdot w_s L_r \sigma I_{dr} - g \frac{M V_s}{L_s} + h_2(x) \end{pmatrix}$$

$$(19) \quad \begin{cases} V_{qr_eq} = -\frac{L_s L_r \sigma}{M \cdot V_s} \dot{P}_s^{ref} + R_r I_{qr} + \\ + g \cdot w_s L_r I_{dr} + g \frac{M \cdot V_s}{L_s} + h_2(x) \\ V_{qr_N} = k \cdot \text{sign}(s(p)) \end{cases}$$

$$(20) \quad \begin{aligned} V_{qr} = & -\frac{L_s L_r \sigma}{M \cdot V_s} \dot{P}_s^{ref} + R_r I_{qr} + g \cdot w_s L_r \sigma I_{dr} + \\ & + g \frac{M \cdot V_s}{L_s} + h_2(x) + k \cdot \text{sign}(s(p)) \end{aligned}$$

b) Reactive Power Control

In order to derive the reactive power regulation rule, the same protocol is followed. The associated expressions are then given below:

$$(21) \quad s(Q) = (I_{dr}^{ref} - I_{dr})$$

$$(22) \quad \dot{s}(Q) = (\dot{I}_{dr}^{ref} - \dot{I}_{dr})$$

By replacing \dot{I}_{dr}^{ref} and \dot{I}_{dr} with their relative expressions, we get:

$$(23) \quad \dot{s}(Q) = \begin{pmatrix} \left(\frac{V_s}{w_s \cdot M} - \frac{L_s}{V_s \cdot M} \dot{Q}_s^{ref} \right) + \\ -\frac{1}{L_r \sigma} (V_{dr} - R_r \cdot I_{dr} + g \cdot w_s L_r \sigma I_{qr} + h_1(x)) \end{pmatrix}$$

$$(24) \quad \dot{s}(Q) = \begin{pmatrix} \left(\frac{V_s}{w_s \cdot M} - \frac{L_s}{V_s \cdot M} \dot{Q}_s^{ref} \right) - \frac{1}{L_r \sigma} V_{dr} + \\ -\frac{1}{L_r \sigma} (-R_r I_{dr} + g w_s L_r \sigma I_{qr} - h_1(x)) \end{pmatrix}$$

$$(25) \quad \begin{aligned} V_{dr} = & L_r \sigma \left(\frac{V_s}{w_s \cdot M} - \frac{L_s}{V_s \cdot M} \dot{Q}_s^{ref} \right) + R_r I_{dr} + \\ & - g w_s L_r \sigma I_{qr} + h_1(x) + k \cdot \text{sign}(s(Q)) \end{aligned}$$

$$(26) \quad \begin{cases} V_{dr_eq} = L_r \sigma \left(\frac{V_s}{w_s M} - \frac{L_s}{V_s M} \dot{Q}_s^{ref} \right) + \\ \quad + R_r I_{dr} - g w_s L_r \sigma I_{qr} + h_1(x) \\ V_{dr_N} = k \cdot \text{sign}(s(Q)) \end{cases}$$

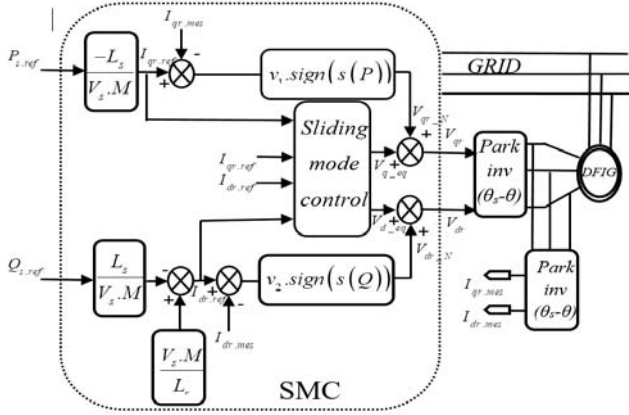


Fig1. Block diagram of SMC applied to DFIG

4. DFIG Faulty model

In this part, a DFIG model is built in the event of rotor and stator faults, which can be of mechanical and electrical nature. According to [16], the occurrence of these faults generates asymmetry in the DFIG and causes harmonics in the stator windings. Thus, the stator current components are augmented by a sinusoidal factor of pulsation $\omega_i = 2\pi f_i$.

The sinusoidal components caused by the occurrence of faults can be represented by the ecosystem as follows [27-28].

$$(27) \quad \dot{w} = S(w) \cdot w \quad w \in \mathfrak{R}^{4n_f+2}$$

With

$$w = (\omega_1 \quad \omega_{-1} \quad \dots \quad \omega_{n_f} \quad \omega_{-n_f})$$

Where

w : The pulsations vector, n_f : The number of broken bars faults.

$$S(w) = \text{diag}(S_{r,1}, \dots, S_{r,n_f})$$

$$S_{r,k} = \text{diag} \left(\begin{pmatrix} 0 & \omega_k \\ -\omega_k & 0 \end{pmatrix}, \begin{pmatrix} 0 & \omega_{-k} \\ -\omega_{-k} & 0 \end{pmatrix} \right)$$

Where $\omega_{\pm k}, k = 1, \dots, n_f$: are the pulsations of the harmonics caused by the rotor faults, these faults can be created by rotor asymmetry because broken bars produce harmonics component at the frequency explained in

$$(28) \quad f_{r,k} = (1 \pm 2ks_w) \cdot f$$

Where:

k : Positive integer ($k = 1, \dots, n_f$)

s_w : The slip ($s_w = \omega_s - \omega$), f : The supply frequency.

The harmonics' amplitudes and phases depend on the ecosystem's initial state $w(0)$ of the ecosystem. Then, the additive sinusoidal terms can be as a suitable combination of the ecosystem state, i.e.:

$$(29) \quad \begin{cases} i_{sd} \rightarrow i_{sd} + Q_d w \\ i_{sq} \rightarrow i_{sq} + Q_q w \end{cases}$$

With

$$\begin{cases} Q_d = (1 \quad 0 \quad 1 \quad 0 \quad \dots \quad 1 \quad 0) \\ Q_q = (0 \quad 1 \quad 0 \quad 1 \quad \dots \quad 0 \quad 1) \end{cases}$$

The derivative of (29) is given by:

$$(30) \quad \begin{cases} \frac{dI_{ds}}{dt} \rightarrow \frac{dI_{ds}}{dt} + Q_d \cdot S \cdot w \\ \frac{dI_{qs}}{dt} \rightarrow \frac{dI_{qs}}{dt} + Q_q \cdot S \cdot w \end{cases}$$

After inserting the additive perturbing terms $Q_d w, Q_q w$ and their derivatives $Q_d \cdot S \cdot w, Q_q \cdot S \cdot w$ respectively, we get the defective model of DFIG by the following state equations:

$$(31) \quad \begin{cases} \frac{dI_{ds}}{dt} = -a_0 I_{ds} + b_1 \omega_s I_{qs} - a_1 I_{qs} + a_2 R_r I_{dr} + \\ \quad - a_3 \omega_r I_{qr} + a_3 \omega_s I_{qr} + b_0 V_{ds} - a_2 V_{dr} + \Gamma_{ds} \cdot w \\ \frac{dI_{qs}}{dt} = -a_0 I_{qs} + b_1 \omega_s I_{ds} + a_1 \omega_r I_{ds} + a_3 \omega_r I_{dr} + \\ \quad + a_2 R_r I_{qr} - a_3 \omega_s I_{dr} + b_0 V_{qs} - a_2 V_{qr} + \Gamma_{qs} \cdot w \\ \frac{dI_{dr}}{dt} = a_5 I_{ds} - a_6 \omega_s I_{qs} + a_6 \omega_r I_{qs} - b_2 R_r I_{dr} + \\ \quad + b_1 \omega_r I_{qr} - a_4 \omega_s I_{qr} - a_7 V_{ds} + b_2 V_{dr} + \Gamma_{dr} \cdot w \\ \frac{dI_{qr}}{dt} = a_6 \omega_s I_{ds} - a_6 \omega_r I_{ds} + a_5 I_{qs} + a_4 \omega_s I_{dr} + \\ \quad - b_1 \omega_r I_{dr} - b_2 R_r I_{qr} - a_7 V_{qs} + b_2 V_{qr} + \Gamma_{qr} \cdot w \end{cases}$$

Where: $x = [I_{ds} \quad I_{qs} \quad I_{dr} \quad I_{qr}]^T$, $\Gamma_{ds}, \Gamma_{qs}, \Gamma_{dr}$ and Γ_{qr}

describe the fault terms, presented by:

$$\begin{cases} \Gamma_{ds} = -a_0 Q_d + b_1 \omega_s Q_q - a_1 Q_q - Q_d S \\ \Gamma_{qs} = -a_0 Q_q + b_1 \omega_s Q_d - a_1 \omega_r Q_q - Q_q S \\ \Gamma_{dr} = a_5 Q_d + a_6 \omega_s Q_q + a_6 \omega_r Q_q \\ \Gamma_{qr} = a_6 \omega_s Q_d - a_6 \omega_r Q_d + a_5 Q_q \end{cases}$$

5. ILC scheme

Iterative learning control method is used to enhance the monitoring performance of repetitively operating machines over a set length of time. It is beneficial for problems where a system must follow several types of inputs in the face of design, modelling unreliability, or repeated disturbances in input as a comeback to system nonlinearities. ILC maintains the preceding output and error information as a memory, as well as an error correction algorithm.

In the time domain, the proposed ILC scheme is shown in Fig. 2, with the following learning law:

$$(32) \quad u_{i+1}(t) = (1 - \alpha)u_i(t) + \Phi e_i(t) + \Gamma e_{i+1}(t)$$

where: $u_i(t)$ is the control signal that was generated from ILC, $i = 1, 2, 3, \dots$ is the iteration number, $e_i(t)$ is the active

power error signal with $p_s^*(t) - p_s(t)$, α is the forgetting factor, Γ and Φ are the previous and current cycle feedback gains, respectively. (See [17-18] for more information about determining the learning gains and). Fig. 3 shows the overall block diagram of the system and the proposed control strategy (SMC-ILC).

When the system is vulnerable to significant disruptions that can deteriorate the overall system performance. Therefore, based on the ILC, the suggested approach changes the input control trajectories when the control operation is repeated to achieve zero tracking error. Meanwhile, the suggested ILC controller exploits undesirable output voltage disturbances whose frequencies are encompassed within the sliding controller's bandwidth.

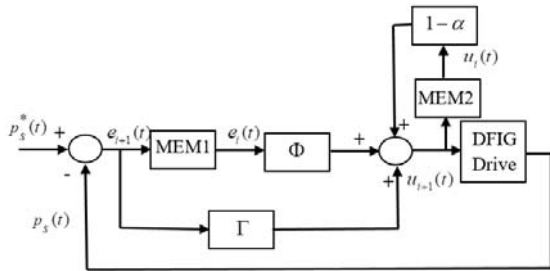


Fig. 2. Block diagram of the ILC approach applied in the time domain.

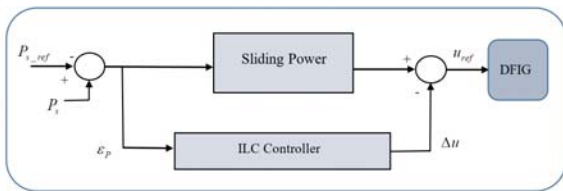


Fig. 3 Overall block diagram of the system and the proposed control strategy.

6. Simulation and interpretation

To validate the performance of the proposed scheme mentioned in the previous section, we present a series of computer simulations for a doubly-fed induction generator whose nominal electrical and mechanical parameters are shown in Table 1. We use MATLAB/Simulink to build the simulation.

Table 1. Parameters of the DFIG adopted for the experimental activity.

Parameters	Values	Units
R_s	0.455	Ω
R_r	0.6	Ω
L_s	0.084	H
L_r	0.081	H
L_m	0.078	H
J	0.3125	$Kg.m^2$
P	2	-
F	0	$N.m/rad/s$

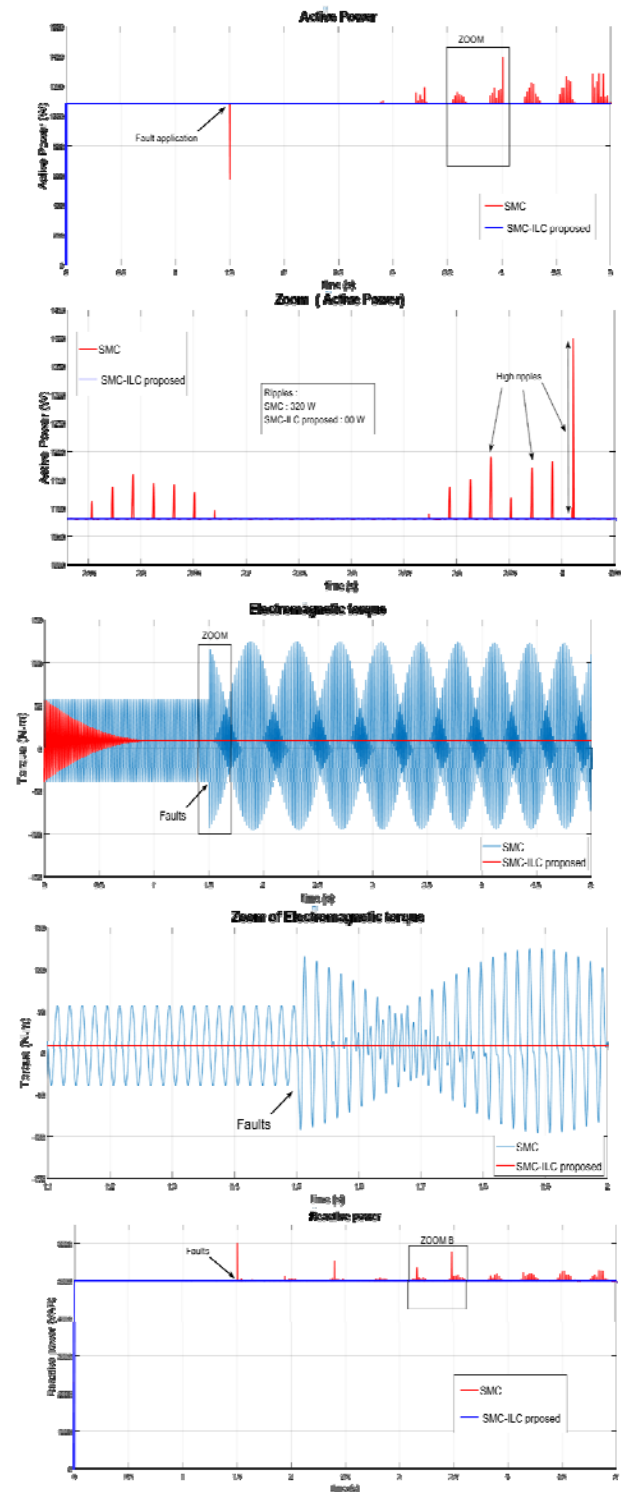
Figures 05 shows the efficiency of the proposed control FTC (SMC-ILC) compared to the traditional SMC with different modes of operation, especially in post-fault operation.

Table 2. Comparative results between SMC and SMC-ILC when the fault occurs

Characteristics	SMC	SMC-ILC
Ripples of active power (W)	>300	Disappear
Ripples of reactive power (VAR)	>700	Disappear
Ripples of I_{dr} (A)	> 4.5	Disappear
Ripples of I_{qr} (A)	>5.1	Disappear

Depending on Fig.5 and Table.2, which shows the performance of the traditional SMC and the proposed SMC-ILC in faulty conditions, we notice that:

- The ripples almost disappeared in the signals of active and reactive power, with the proposed SMC-ILC compared to the classical SMC in which the ripples are up to 300 W in active power and 700 VAR in reactive power.
- The ripples in the Direct and quadratic current signal are also eliminated with the suggested technique; for example, the ripples of the Direct rotor current reached 4.5 A, and the ripples of the quadratic rotor current exceeded 5.1 A.
- The response time and overshoot of the electromagnetic torque are improved by the proposed SMC-ILC controller more than by conventional SMC.



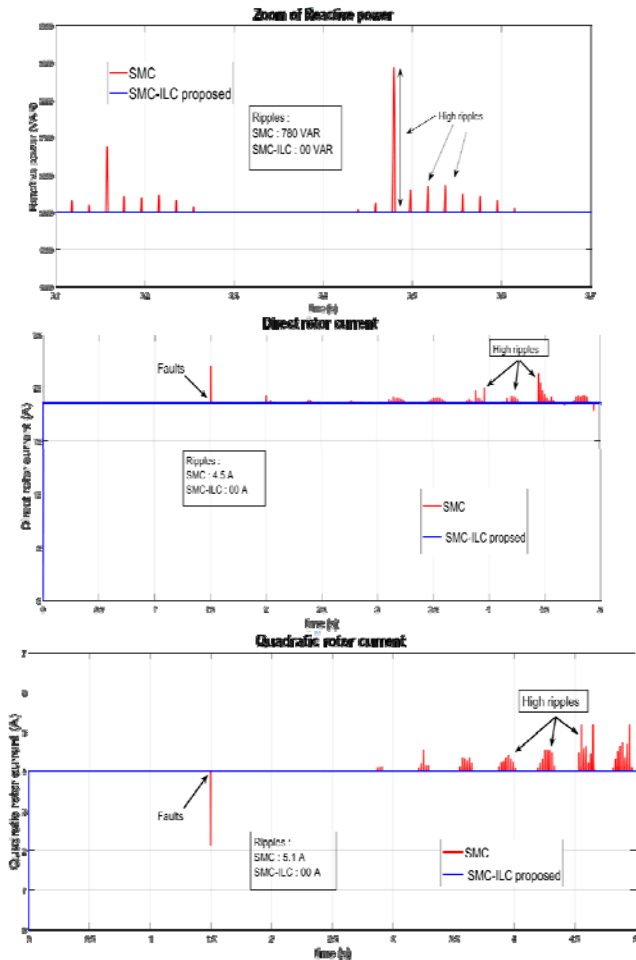


Fig.5 Performances of the SMC and SMC-ILC in faulty condition

6.1. Robustness test

In order to test the robustness of the proposed control schemes, the value of rotor inductance L_r is increased by 10% and 20% of their nominal value, Fig.6 and Fig.7, show the effects of parameters variation on the active and reactive power responses for the SMC and SMC-ILC controllers.

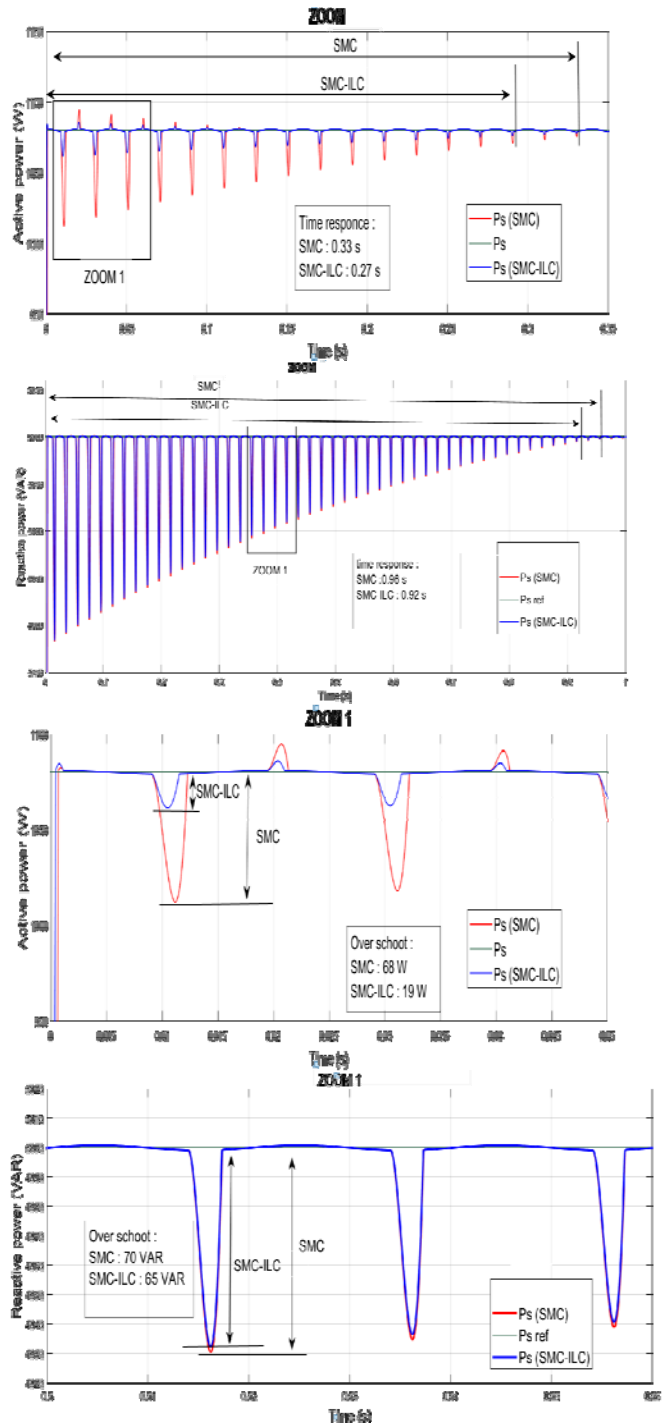
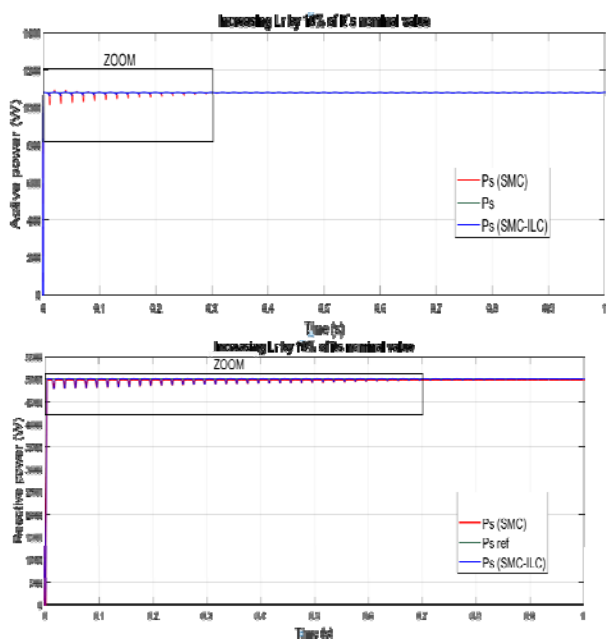


Fig.6. Active and Reactive power behaviour using SMC and SMC-ILC controllers with 10% variation of L_r

Table.3 summarizes the main improvement of the proposed SMC-ILC compared to conventional SMC in the face of variation of the rotor inductance L_r . We can notice that: In the first case (when the L_r increases by 10% of its nominal value):

- The Active power response time (s) is reduced for conventional SMC from 0.33s to 0.27s using the proposed SMC-ILC so enhancement for 18 %.
- The Active power overshoot is reduced by more than 72 % (68 W for conventional SMC instead 19W for proposed SMC-ILC).
- The response time (s) of the Reactive power is reduced for conventional SMC from 0.96s to 0.92s using the proposed SMC-ILC).

- The Reactive power overshoot is reduced by more than 07% (70 VAR for conventional SMC instead of 65 VAR for the proposed SMC-ILC).
- In the second case (when the Lr increases by 20% of its nominal value):
- Active power response time is reduced by more than 9.5% (13,6s for conventional SMC instead of 12.3s for the proposed SMC-ILC).
 - the Active power overshoot is reduced by more than 82% (280 W for SMC instead 50W for proposed SMC-ILC)
 - Reactive power response time is reduced by more than 19.3% (1.45s for conventional SMC instead of 1.17s for the proposed SMC-ILC).
 - the Reactive power overshoot is reduced by more than 28% (125 VAR for SMC instead of 90VAR for the proposed SMC-ILC)
 - SMC-ILC)

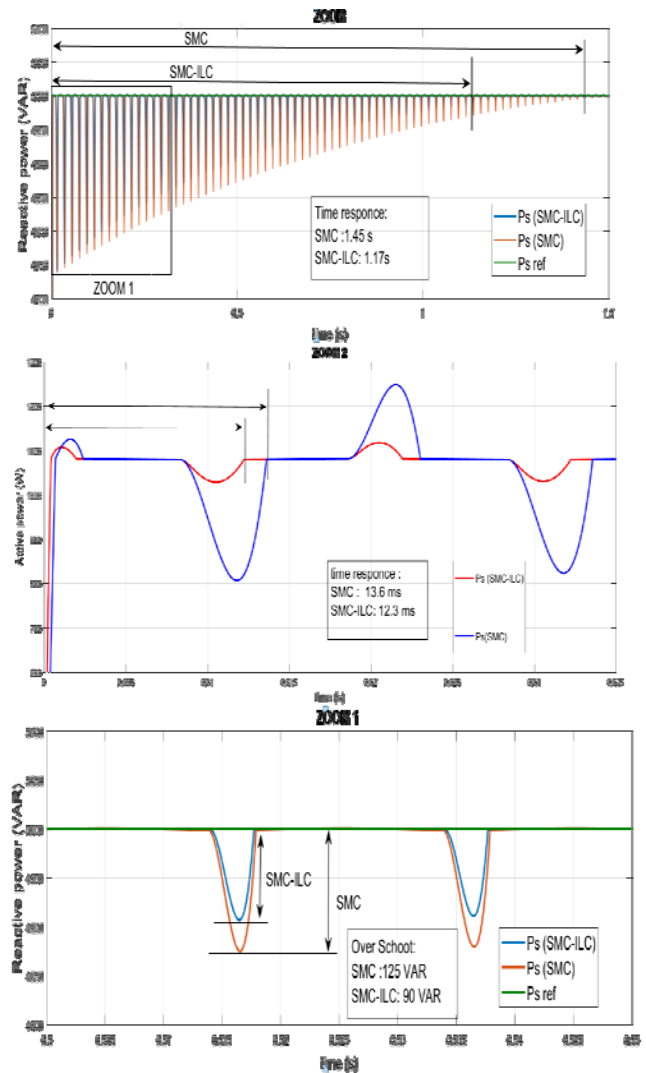
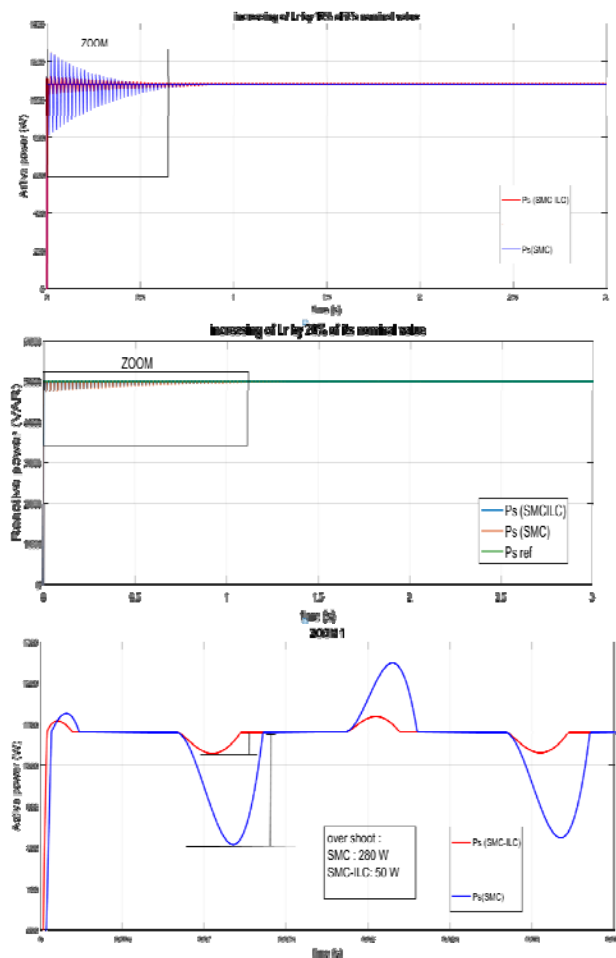


Fig.7. Active and Reactive power behaviour using SMC and SMC-ILC controllers with 20% variation of Lr

From Figures. 5-6-7 and Tables 2-3, the significant contributions of this work are:

1. the improvement of the response time,
2. the reduction of the ripple and overshoot,
3. the ability of the proposed SMC-ILC to compensate for the faults.

Therefore, the proposed SMC-ILC guarantees a better response with precise reference tracking, almost as in the case of a healthy operation.

Table .3. Comparative results between SMC and SMC-ILC with Lr variation

Characteristics	SMC	Variation of Lr (10% of nominal value)		Variation of Lr (20% of nominal value)			
		SMC-ILC	improvement reduction ratio %	SMC	SMC-ILC	improvement reduction ratio %	
P _s	Time response (s)	0.33	0.27	18	13.6	12.3	9.5
	Overshoots (W)	68	19	72	280	50	82
Q _s	Time response (s)	0.96	0.92	04	1.45	1.17	19.3
	Overshoots (VAR)	70	65	07	125	90	28

7. Conclusion

This paper has proposed a sliding mode control (SMC) and an iterative learning control (ILC) for Doubly-Fed Induction Generator. The proposed FTC (SMC-ILC) is based on combining a Sliding Mode Controller (SMC) with an Iterative Learning Controller (ILC) to eliminate the effect of rotor faults. Learning control is intuitively an excellent selection for power ripple minimization. In addition, the scheme does not need any correct information of the motor parameters as it also could be attached to any controller due to the easy implementation process. In the event of fault, Simulation results and Table 2 demonstrate the enhancement of the power quality, effectiveness and high robustness of the proposed SMC-ILC compared to old SMC. For when the industrial power quality and the operating circumstances are in a critical condition, the proposed control can be significantly useful to preserve such problems.

Authors: Oussama djaidja, Dr. Hemza Mekki, Dr. Samir Zeghleche, Dr. Ali Djerioui, Department of Electrical Engineering, Faculty of Technology, University Mohamed Boudiaf of M'Sila, BP 166, Ichbilila 28000, Algeria, E-mail:oussama.djaidja@univ-msila.dz

REFERENCES

- [1] Muhammad Shahzad Nazir, Ye Qin Wang, Ali Jafer Mahdi, Xinguo Sun, Chu Zhang and Ahmed N. Abdalla. "Improving the Performance of Doubly Fed Induction Generator Using Fault Tolerant Control—A Hierarchical Approach", *Appl. Sci.*, vol10 (2020), pp924
- [2] Samir ABDELMALEK, Linda BARAZANE, Abdelkader LARABI, "An advanced robust fault-tolerant tracking control for a doubly fed induction generator with actuator faults", *Turk J Elec Eng & Comp Sci*, vol25 (2017), pp 1346 – 1357
- [3] Riyadh Rouabhi, Rachid Abdessamed, Aissa Chouder, Ali Djerioui, "Power Quality Enhancement of Grid Connected Doubly-Fed Induction Generator Using Sliding Mode Control", *International Review of Electrical Engineering (IREE)*, Vol. 10 (2015), N. 2, pp266-276
- [4] A. Hasni, "Contribution a l'étude et l'analyse de la gestion optimisée du microclimat d'une serre horticole.", Doctorate theses, University of Bechar (Algeria), 2010
- [5] Li-Ying Hao, Guang-Hong Yang, "Robust fault tolerant control based on sliding mode method for uncertain linear systems with quantization", *ISA Transactions*, 2013
- [6] Nouredine Layadi, Samir Zeghlache, Ali Djerioui Hemza Mekki, Fouad Berrabah, Azeddine Houari and Mohamed-Fouad Benkhoris. "Backstepping Fault Tolerant Control for Double Star Induction Machine under Broken Rotor Bars" *Majlesi Journal of Electrical Engineering*, vol13 (2019) (3), pp60-68.
[7] Nouredine Layadi, Ali Djerioui, Samir Zeghlache, Hemza Mekki, Azeddine Houari, Jinlin Gong, Fouad Berrabah, "Fault-Tolerant Control Based on Sliding Mode Controller for Double-Star Induction Machine", *Arabian Journal for Science and Engineering*, 2019
- [8] Prashant. M, Jinfeng. L, Panagiotis. DC. "Fault-tolerant process control methods and applications". London: Springer-Verlag, 2013.
- [9] Nouredine Layadi, Ali Djerioui, Samir Zeghlache, Hemza Mekki, Azeddine Houari, Mohamed, Fouad Benkhoris, Fouad Berrabah, "New Fault Tolerant Control Based On Backstepping Controller For Double Star Induction Machine", *Rev. Roum. Sci. Techn. – Électrotechn. et Énerg.* Vol. 64, 3 (2019), pp. 275–280
- [10] R. Nikoukhah, S.L. Campbell and K. Drake, "An active approach for detection of incipient faults", *International Journal of Systems Science*, Vol. 41, No. 2, February 2010, 241–257
- [11] Zina. H.B, Allouche. M, Souissi. M, Chaabane. M, Chrif. Alaoui.L, "Robust sensor fault-tolerant control of induction motor driver". *Int. J. Fuzzy Syst.* 19(1) (2017), 155–166
- [12] Djeghali. N, Ghanes M, Djennoune S, Barbot JP. Sensorless fault tolerant control for induction motors. *Int. J. Control., Autom. Syst.* 11(3) (2013), pp563–576.
- [13] Boucheta, A, Bousserhane, I.K., Hazzab, A, Mazari, B., Fellah, M.K. (2009). Fuzzy-Sliding Mode Controller for Linear Induction Motor Control. *Rev. Roum. Sci. Techn. – Électrotechn. Et Énerg.*, 54(4): 405-414.
- [14] Bouguerra, A., Zeghlache, S., Loukal, K., Saigaa, D. (2016). Fault Tolerant Fuzzy Sliding Mode Controller of Brushless DC Motor (BLDC MOTOR). *the Mediterranean Journal of Measurement and Control*, 12(2): 585-597.
- [15] Rubagotti M, Castañós F, Ferrara A, Fridman L. Integral sliding mode control for nonlinear systems with matched and unmatched perturbations. *IEEE Trans. Autom. Control.* 2011 ,56(11) 2699–704.
- [16] Mekki H, Benzineb O, Boukhetala D, Tadjine M, Benbouzid M, "Sliding mode based fault detection, reconstruction and fault tolerant control scheme for motor systems", *ISA Trans*, 57 (2015), pp 340– 351
- [17] Qian, W, Panda, S. K, Xu, J.X: 'Speed ripple minimization in PM synchronous motor using iterative learning control', *IEEE Trans. Energy Convers.*, 20 (2005), pp. 53–61
- [18] Azeddine Houari, Ali Djerioui, Abdelhakim Saim, Mourad Ait-Ahmed1, Mohamed Machmoum1: "Improved control strategy for power quality enhancement in standalone systems based on four-leg voltage source inverters" *The Institution of Engineering and Technology* 2017.
- [19] A. Fekih, Effective fault tolerant control design for nonlinear systems: application to a class of motor control system, *IET Control Theory & Applications* 2, (2008) pp762–772
- [20] Gouichiche Abdelmadjid, Boucherit Seghir Mohamed, Tadjine Mohamed, Safa Ahmed, Messlem Youcef, "An improved stator winding fault tolerance architecture for vector control of induction motor: Theory and experiment", *Electric Power Systems Research*, 104 (2013) 129–137
- [21] I. González-Prieto, M. J. Duran, F. J. Barrero, "Fault-Tolerant Control of Six-Phase Induction Motor Drives with Variable Current Injection," *IEEE Transactions on Power Electronics*, Vol. 32:10 (2017), pp. 7894-7903
- [22] E. A. Mahmoud, A. S. Abdel-Khalik, H. F. Soliman, "An Improved Fault Tolerant for A Five-Phase Induction Machine under Open Gate Transistor Faults," *Alexandria Engineering Journal*, Vol. 55:3 (2016), pp. 2609-2620
- [23] T. Mesbahi, T. Ghennam, E.M. Berkouk. A Doubly Fed Induction Generator for Wind Stand-Alone Power Applications (Simulation and Experimental Validation) 978, (2012) pp. 2028-2033, IEEE.
- [24] Edwards C, Spurgeon S. Sliding mode control: theory and applications. London: Taylor & Francis; 1998.
- [25] Utkin V, Guldner J, Shi J. Sliding mode control in electromechanical systems. New York: Taylor & Francis; 1999.
- [26] Shtessel Y, Edwards C, Fridman L, Levant A. Sliding mode control and observation. New York: Springer science +Business media; 2014.
- [27] Bonivento C, Isidori A, Marconi L, Paoli A. Implicit fault tolerant control: application to induction motors. *Automatica* (2004) ,40 (3) 355–71.
- [28] Mekki H., Benzineb O., Boukhetala D., Tadjine M. Fault tolerant control based sliding mode application to induction motor. In: *Proceedings of the International Conference on Control, Engineering & Information Technology, CEIT0 13, Sousse, Tunisia, June 2013*